(Received 29 June 2023, Accepted 27 November 2023, Scheduled 23 January 2024)

# Exploring Interferences Arising in the Construction of GPR Responses from an Object Buried between Two Rough Surfaces by GPILE Method

Marc Songolo[1, *], Nicolas Pinel[2, 3], and Christophe Bourlier[3]

[1] *University of Lubumbashi, Lubumbashi, Democratic Republic of the Congo*
[2] *Icam Ouest School of Engineering — Nantes Campus, Carquefou, France*
[3] *IETR, Polytech Nantes, Nantes Université, Nantes, France*

**ABSTRACT:** In this paper, we explore interferences arising in the electromagnetic scattering by an object buried inside a layer with two rough interfaces by using the GPILE method. We show that there are two categories of interferences in the echoes that make up GPILE: the interferences that are present whatever the chosen scenario and those that come from the geometry of the problem (distance between the three scatterers). In this last category, we can cite for example the interferences which come from the position of the object, more precisely from its depth, because an object closer to one of the surfaces would produce echoes which arrive almost at the same time as those of the nearby interface.

## 1. INTRODUCTION

The scattering of electromagnetic waves by a rough interface has attracted much interest within the physics community in recent decades. Several works devoted to this study have contributed to the development of different resolution methods. First analytical, then numerical thanks to the development of computer science, these methods have made great progress over the decades. The main purpose of this study remains the resolution of Maxwell's equations.

The most widely used numerical method is probably the Finite Difference Time Domain method (FDTD), introduced by Yee [1]. This is the method that has been adopted by gprMax simulation software for GPR (Ground Penetrating Radar) numerical EM simulation [2]. The FDTD method is a direct numerical approximation of the Maxwell equations, where the time and space partial derivatives are approximated by central finite differences. Moreover, the FDTD is governed by its stability condition, which states that a maximum allowed time step is limited by a minimum cell size in the computational domain. This means that the use of a small space sampling induces a small time step. Thus, the FDTD method cannot efficiently simulate complex geometries such as complex-shape objects or random rough surfaces without having to apply a refined space sampling, which all the more increases the computational cost. Another problem, related to the nature of the Yee scheme, is the numerical dispersion.

To overcome this deficiency, we choose here to use an integral boundary equation method, in which the numerical resolution uses the Method of Moments (MoM). Indeed, the MoM discretizes the boundaries (here, the interfaces), whereas the FDTD discretizes the space. The MoM makes then possible to exactly follow the interface profile without any space sampling bias and does not have to refine the space sampling step, which sensitively reduces the numerical complexity. However, when studying the time-domain response, the MoM requires to compute a number of frequency responses and to compute an IFFT. Besides, this method is much better adapted to homogeneous media.

In the case of scattering by several rough surfaces, the number of unknowns increases, and the impedance matrix becomes large, which gives particular interest to rapid methods. Some methods have been devoted to obtaining a rigorous solution. We will cite for example the PILE (Propagation-Inside-Layer Expansion) method [3] for the scattering by two superimposed surfaces or an object buried under a surface. This method have a simple mathematical formulation and an intuitive physical interpretation. In the PILE method, the inversion of the impedance matrix results in an iterative process, in the form of an expansion series which takes into account the multiple reflections of the wave in the layer. Subsequently, the EPILE method was developed to deal with the more general case of scattering from two illuminated scatterers [4].

Following these work, the EPILE method was adapted to the case of more than two scatterers. Several methods already related to the case of three scatterers, especially in the study of scattering by two objects buried under a rough surface [5, 6] or an object buried between two surfaces [7]. Thus, the EPILE method was combined with the Forward-Backward (FB) to the case of several objects located above a rough surface in [8]. Next, the EPILE method was combined with FB to the problem of scattering by two objects, one above and the other below a rough surface in [9, 10].

* Corresponding author: Marc Songolo (marc.songolo@gmail.com).

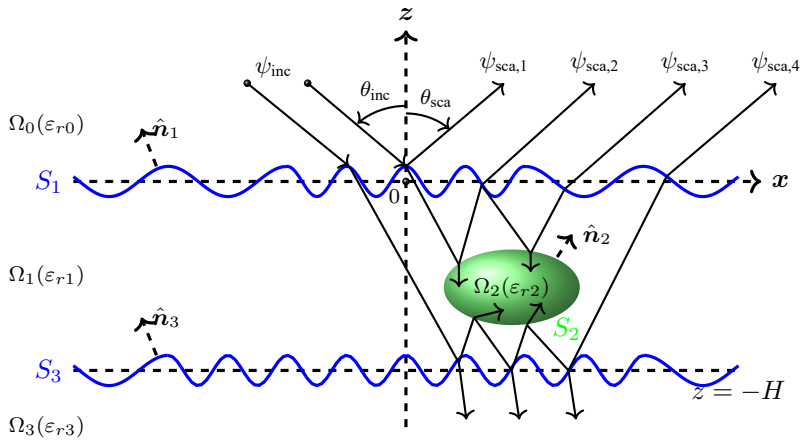


**FIGURE 1**. Electromagnetic scattering from an object buried between two 1-D rough surfaces (2-D problem: plane $(\hat{\boldsymbol{x}}, \hat{\boldsymbol{z}})$).

In the same spirit, the PILE method has been extended to a more general case of the scattering from three superimposed surfaces to obtain a generalization of the PILE method (GPILE: Generalized PILE) [11]. More recently, the GPILE method have been developped to generalize the PILE and EPILE methods to the case of scattering by an object buried between two rough surfaces [12]. The obtain results make it possible to distinguish the primary echo from the upper surface and the multiple echoes coming from the lower surface and the object. Thus, the GPILE method improves the understanding of the wave scattering mechanism in complex medium. The main difference between the problem of three superimposed surfaces treated in [11] and that of an object buried between two surfaces (which is treated here) concerns the last case, for which the two buried scatterers are both illiminated by the wave transmitted by the upper surface.

One of the important phenomena in the study of electromagnetic scattering in a complex medium is the analysis of interferences between echoes from different scatterers. Indeed, it was established in [12] that the nature of the GPR signal depends not only on the physical and geometrical parameters of the interfaces, but also on the interferences between the echoes of the scatterers. Thus, the objective of this paper is to use the GPILE method to explore the interferences between the echoes which constitute the GPR signal for the case of an object buried between two rough surfaces.

In what follows, we first expose in Section 2 the GPILE method as well as its physical interpretation. We then present the different sources at the origin of interferences between the echoes of the three scatterers in Section 3. Several simulations show the effects of these interferences on the overall signal of the GPR response in Section 4.

## 2. GPILE METHOD

Consider in Fig. 1 a 2D problem, with two random rough surfaces $S_1$ and $S_3$ and an object delimited by the surface $S_2$ buried between the interfaces $S_1$ and $S_3$. We assume that the surfaces do not intercept each other or the object. The three interfaces separate four homogeneous media: the upper medium, $\Omega_0$, assumed to be vaccum, the intermediate medium, $\Omega_1$, which constitutes a layer, the buried object which constitutes the medium $\Omega_2$, and the lower medium, $\Omega_3$, which we consider to be dielectric. Consider an incident wave $\psi_{\text{inc}}(\boldsymbol{r})$ in the plane $(\hat{\boldsymbol{x}}, \hat{\boldsymbol{z}})$, at an incidence angle $\theta_{\text{inc}}$ defined relatively to the axis $\boldsymbol{z}$ counterclockwise.

The integral equation method allows to calculate the currents and their normal derivatives on the surfaces $S_i$ $(i = \{1, 2, 3\})$ and to deduce the scattering fields in each medium by using Huygens' principle. The obtain integral equations (two equations per interface) are discretized by the MoM at each interface and leading to the linear system $\bar{\boldsymbol{Z}}\boldsymbol{X} = \boldsymbol{b}$, where the impedance matrix is [13]:

$$\bar{\boldsymbol{Z}} = \begin{pmatrix} \bar{\boldsymbol{Z}}_{11} & \bar{\boldsymbol{Z}}_{21} & \bar{\boldsymbol{Z}}_{31} \\ \bar{\boldsymbol{Z}}_{12} & \bar{\boldsymbol{Z}}_{22} & \bar{\boldsymbol{Z}}_{32} \\ \bar{\boldsymbol{Z}}_{13} & \bar{\boldsymbol{Z}}_{23} & \bar{\boldsymbol{Z}}_{33} \end{pmatrix}. \tag{1}$$

The impedance matrix is of size $2(\sum_{i=1}^{3} N_i) \times 2(\sum_{i=1}^{3} N_i)$, where $N_i$ is the number of samples on $S_i$. The unknown vectors $\boldsymbol{X}_i$ containing the surface currents and their normal derivatives are written as

$$\boldsymbol{X}_i = \left[\psi_i(\boldsymbol{r}_1) \cdots \psi_i(\boldsymbol{r}_{N_i}) \quad \frac{\partial \psi_i(\boldsymbol{r}_1)}{\partial n_i} \cdots \frac{\partial \psi_i(\boldsymbol{r}_{N_i})}{\partial n_i}\right]^T, \tag{2}$$

where $\boldsymbol{r}_{p\in[1;N_i]} \in S_i, i = \{1, 3\}$ for the two surfaces, and $\boldsymbol{r}_{p\in[1;N_2]} \in S_2$ for the object. The right term $\boldsymbol{b}$ is the incident field:

$$\boldsymbol{b} = [\boldsymbol{b}_1 \quad \boldsymbol{b}_2 \quad \boldsymbol{b}_3]^T. \tag{3}$$

To calculate the currents on the three interfaces, we may extend the PILE method [3] to the case of three scatterers (where only one is illuminated by the incident field) by coupling the upper surface and the object plus the lower surface as a single composite scatterer, then split up the object and the lower surface in the spirit of PILE method. By this way, the calculation of the currents on the upper surface makes it possible to obtain [12]:

$$\boldsymbol{X}_1 = \sum_{p=0}^{P} \left( \sum_{q=0}^{Q} \bar{\boldsymbol{M}}_{c,21}^{(q)} + \sum_{q=0}^{Q} \bar{\boldsymbol{M}}_{c,31}^{(q)} \right)^p \bar{\boldsymbol{Z}}_{11}^{-1} \boldsymbol{b}_1, \tag{4}$$

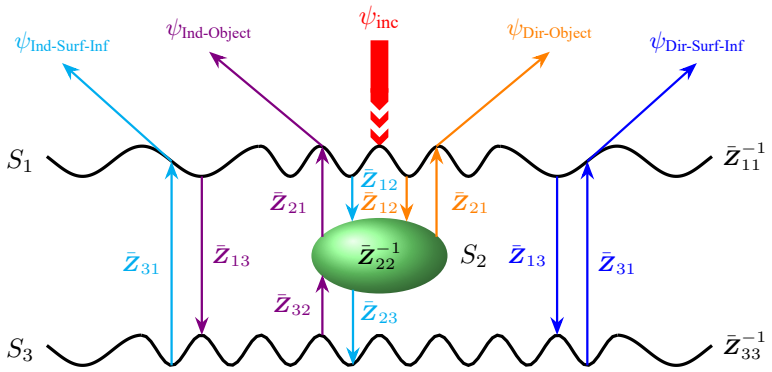


**FIGURE 2**. Graphic representation of the contributions of the object and the lower surface. The direct and indirect contributions of the object are respectively denoted: $\psi_{\text{Dir-Object}}$ and $\psi_{\text{Ind-Object}}$. Those of the lower surface are respectively denoted: $\psi_{\text{Dir-Surf-Inf}}$ and $\psi_{\text{Ind-Surf-Inf}}$.

where

$$\sum_{q=0}^{Q} \bar{\boldsymbol{M}}_{c,21}^{(q)} = \bar{\boldsymbol{Z}}_{11}^{-1}\bar{\boldsymbol{Z}}_{21}\left(\sum_{q=0}^{Q}\bar{\boldsymbol{M}}_{c,32}^{q}\right)\bar{\boldsymbol{Z}}_{22}^{-1}\left(\bar{\boldsymbol{Z}}_{12}-\bar{\boldsymbol{Z}}'_{12}\right), \tag{5}$$

and

$$\sum_{q=0}^{Q} \bar{\boldsymbol{M}}_{c,31}^{(q)} = \bar{\boldsymbol{Z}}_{11}^{-1}\bar{\boldsymbol{Z}}_{31}\left(\sum_{q=0}^{Q}\bar{\boldsymbol{M}}_{c,23}^{q}\right)\bar{\boldsymbol{Z}}_{33}^{-1}\left(\bar{\boldsymbol{Z}}_{13}-\bar{\boldsymbol{Z}}'_{13}\right). \tag{6}$$

In expression (5), the matrix

$$\bar{\boldsymbol{M}}_{c,32} = \bar{\boldsymbol{Z}}_{22}^{-1}\bar{\boldsymbol{Z}}_{32}\bar{\boldsymbol{Z}}_{33}^{-1}\bar{\boldsymbol{Z}}_{23} \tag{7}$$

is one of the two characteristic matrices between the two buried scatterers. This matrix brings the contributions from the lower surface to the object. As for the matrix $\bar{\boldsymbol{Z}}'_{12} = \bar{\boldsymbol{Z}}_{32}\bar{\boldsymbol{Z}}_{33}^{-1}\bar{\boldsymbol{Z}}_{13}$, it represents the indirect coupling between the upper surface and the object via the lower surface. In expression (6), the matrix

$$\bar{\boldsymbol{M}}_{c,23} = \bar{\boldsymbol{Z}}_{33}^{-1}\bar{\boldsymbol{Z}}_{23}\bar{\boldsymbol{Z}}_{22}^{-1}\bar{\boldsymbol{Z}}_{32} \tag{8}$$

is the other characteristic matrix between the two buried scatterers and brings the contributions of the object to the lower surface. The matrix $\bar{\boldsymbol{Z}}'_{13} = \bar{\boldsymbol{Z}}_{23}\bar{\boldsymbol{Z}}_{22}^{-1}\bar{\boldsymbol{Z}}_{12}$ represents the coupling matrix between the two surfaces via the object.

The calculation of the currents on the other interfaces allows us to obtain:

$$\boldsymbol{X}_2 = -\left(\sum_{q=0}^{Q}\bar{\boldsymbol{M}}_{c,32}^{q}\right)\bar{\boldsymbol{Z}}_{22}^{-1}\left(\bar{\boldsymbol{Z}}_{12}-\bar{\boldsymbol{Z}}'_{12}\right)\boldsymbol{X}_1 \tag{9}$$

and

$$\boldsymbol{X}_3 = -\left(\sum_{q=0}^{Q}\bar{\boldsymbol{M}}_{c,23}^{q}\right)\bar{\boldsymbol{Z}}_{33}^{-1}\left(\bar{\boldsymbol{Z}}_{13}-\bar{\boldsymbol{Z}}'_{13}\right)\boldsymbol{X}_1. \tag{10}$$

Remark that the orders $P$ and $Q$ are arbitrary. In fact, the principal order $p$ represents the round trips of the wave between the upper surface and the two buried scatterers, while the secondary order $q$ represents the round trips of the wave between the two buried scatterers. Besides, the memory requirement of the GPILE method is the same as that of the LU method, i.e., $(N_1+N_2+N_3)^2$. On the other hand, the complexity in number of operations is $(N_1)^3+(N_2)^3+(N_3)^3$ for the inversion of the impedance matrix by GPILE method instead of $(N_1+N_2+N_3)^3$ for the direct LU method.

## 3. INTERFERENCES

In the case of flat interfaces, the first three echoes for the case without the object occur at times $T_{2,\text{S}}$ and $T_{3,\text{S}}$ defined respectively by:

$$\begin{cases} T_1 = 2z_{\text{obs}}/c \\ T_{2,\text{S}} = T_1 + 2H\text{Re}(\sqrt{\epsilon_{\text{r,1}}}) \\ T_{3,\text{S}} = T_1 + 4H\text{Re}(\sqrt{\epsilon_{\text{r,1}}}) \end{cases} \tag{11}$$

where $c$ is the velocity of light, and $H$ is the thickness of the layer (the average distance between the two surfaces). We can get the times of the second and third echoes for the object by replacing $H$ with $H_{12}$ in the Eq. (11), where $H_{12}$ is the depth of the object. The times of these echoes are written $T_{2,\text{O}}$ and $T_{3,\text{O}}$. Note that the depth of the object is calculated relatively to the center of the object.

All these echoes are calculated for the PILE method. For the GPILE method, we have shown in [12] that the second and third echoes result from multiple scattering between the three scatterers in the intermediate medium. Thus, the second echo for example ($P=1$ and $Q=0$) is made up of one contribution from the object and another one from the lower surface. Each of these contributions has a direct and an indirect component. Fig. 2 shows the contributions of the object and the lower surface. The direct and indirect contributions of the object are respectively denoted: $\psi_{\text{Dir-Object}}$ and $\psi_{\text{Ind-Object}}$. Those of the lower surface are respectively denoted: $\psi_{\text{Dir-Surf-Inf}}$ and $\psi_{\text{Ind-Surf-Inf}}$. Moreover, the echoes of the direct contributions from the two buried scatterers occur at different times, but the echoes of the indirect contributions of these two buried scatterers arrive at the same time, because the wave travels the same

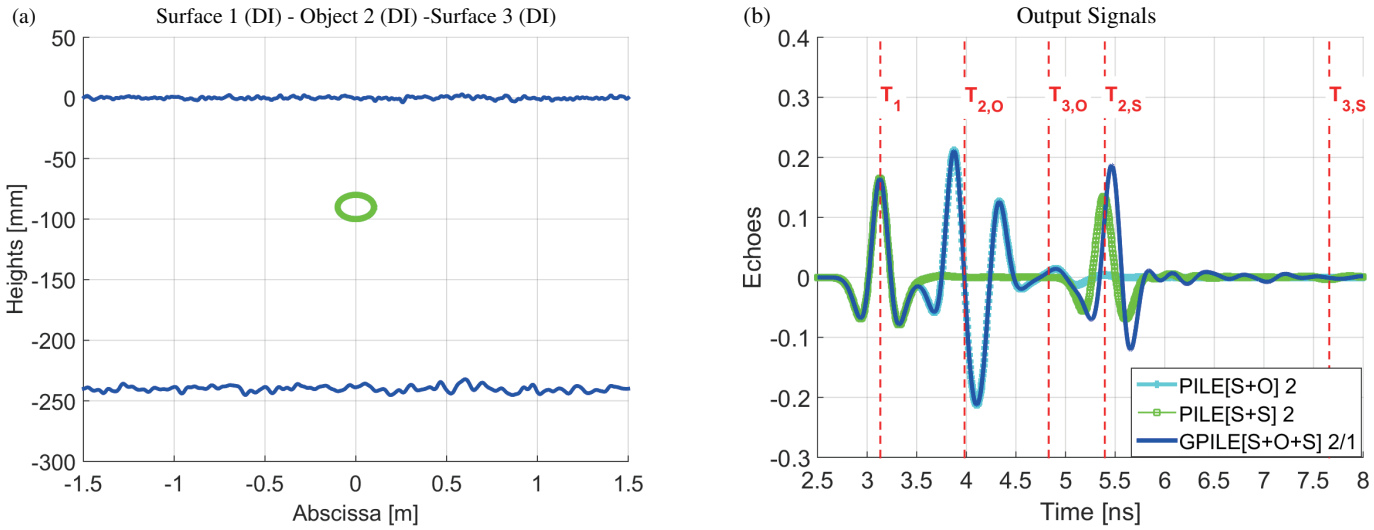


**FIGURE 3**. (a) Surface heights versus their abscissa for Gaussian PDF and ACF, with $\sigma_{\mathrm{h},1} = 1\,\mathrm{mm}$ and $\sigma_{\mathrm{h},3} = 2.5\,\mathrm{mm}$, $L_{\mathrm{ch},1} = 15\,\mathrm{mm}$ and $L_{\mathrm{ch},3} = 30\,\mathrm{mm}$. The center of the elliptical cylinder is $C = (0, -90)\,\mathrm{mm}$, with semi-major axis $a = 100\,\mathrm{mm}$ and semi-minor axis $b = 10\,\mathrm{mm}$. The thickness between the two surfaces $H = 240\,\mathrm{mm}$. (b) Time responses of the scattered field for the scenario described in (a), with $x_{\mathrm{obs}} = 0$ and $z_{\mathrm{obs}} = 470\,\mathrm{mm}$.

distance for the two indirect contributions, although in opposite directions for one relative to the other.

For $Q = 1$, one can add the time for a round trip between the object and the lower surface, given by $T_{\mathrm{OS}} = T_{2,\mathrm{S}} - T_{2,\mathrm{O}}$ (also adding the diffraction time on the two scatterers). We deduce that the direct contribution of the object to the order $Q = 1$ theoretically arrives at the time $T_{2,\mathrm{O}} + T_{\mathrm{OS}} = T_{2,\mathrm{S}}$. Therefore, it is added to the three contributions which already produced interferences around $T_{2,\mathrm{S}}$ for $Q = 0$. The three other contributions to the order $Q = 1$, for their part, arrive at the time $T_{2,\mathrm{S}} + T_{\mathrm{OS}}$.

It is valuable to notice that when the object is very close to the upper surface, $T_{2,\mathrm{O}}$ is close to $T_1$, because $T_{\mathrm{SO}} = T_{2,\mathrm{O}} - T_1$ is very small. Thus, the echo of the direct contribution of the object interferes with the primary echo from the upper surface. If, on the other hand, the object is very close to the lower surface, then $T_{2,\mathrm{O}}$ is close to $T_{2,\mathrm{S}}$, because $T_{\mathrm{OS}}$ is very small. It follows that the direct and indirect contributions of the two scatterers to the order $Q = 0$, and their resultants for the order $Q = 1$ arrive around $T_{2,\mathrm{S}}$, which complicates the analysis of the signal, as we will see later.

Another even more complex scenario is that of an object buried between two surfaces separated by a relatively thin layer. This implies that the buried object is close to both surfaces. Thus, the echoes of the three scatterers will overlap. In such a case, the primary echo from the upper surface interferes with the second echoes from the lower surface and from the object around $T_1$. Similarly, the second echoes from the two buried scatterers interfere around $T_{2,\mathrm{O}}$ and $T_{2,\mathrm{S}}$, which are very close. It therefore follows that we have eight echoes from the two buried scatterers and the primary echo from the upper surface, making a total of nine echoes, which interfere over a reduced time window due to the thinness of the layer.

The phenomenon of interference therefore requires particular care. We can distinguish two categories of interferences in the echoes that make up GPILE: the interferences that are present whatever the chosen scenario and those that come from the geometry of the problem (distance between the scatterers). In the first category, we have for example the interferences between the indirect contributions of the two buried scatterers and the direct contribution of the lower surface, for the same values of $p$ and $q$. To these three contributions we add the contribution of a round trip between the object and the lower surface of the direct contribution of the object. For the second category, we can quote the interference between the primary echo from the upper surface and the second echo of the object, when the object is very close to the upper surface. Similarly, when the object is very close to the lower surface, the echoes from these two contributions interfere with the echoes from the first category. When the buried object is close to both surfaces, i.e., in the case of a relatively thin layer, the multiple echoes of the three scatterers overlap.

## 4. NUMERICAL SIMULATIONS

For the numerical simulations, a Ricker pulse is considered as an input signal [11]. In the time domain, it is defined as

$$s(t) = \left(2\pi^2 f_c^2 t^2 - 1\right) \exp\left(-\pi^2 f_c^2 t^2\right). \tag{12}$$

In the Fourier domain, it is defined as

$$\widehat{s}(f) = -\frac{2f^2}{f_c^3\sqrt{\pi}} \exp\left(-\frac{f^2}{f_c^2}\right), \quad f \geq 0. \tag{13}$$

For our simulations, we consider the central frequency $f_c = 2\,\mathrm{GHz}$; the number of frequencies is $N_f = 117$; and the band is $[0.2 - 6.0]\,\mathrm{GHz}$. We also applied the zero-padding technique to

increase $N_f$ to $2^{12} = 4096$, in order to have a better resolution in the time domain.

To numerically experiment the interferences of the first category, we consider a scenario in which the three scatterers are distant from each other, as shown in Fig. 3(a). Besides, we shall specify the relative permittivity values of the different media: for the upper medium $\epsilon_{r,0} = 1$, for the inner medium $\epsilon_{r,1} = 2$, for the object $\epsilon_{r,2} = 7$, and for the lower medium $\epsilon_{r,3} = 4$. In the numerical simulations, PILE(S+O) represents the scattered field of the object buried under the surface, PILE(S+S) represents the scattered field of the two surfaces (without the object) and GPILE(S+O+S) represents the scattered field of the object buried between the two surfaces. Observe that the electromagnetic response of the object buried between the two surfaces GPILE(S+O+S) and that of the object buried under the surface PILE(S+O) coincide around $T_{2,\mathrm{O}}$ as shown in Fig. 3(b). This is linked to the fact that the direct contribution of the object for GPILE(S+O+S) is exactly PILE(S+O). However, there is a remarkable difference in amplitude between the electromagnetic response of two surfaces PILE(S+S) and that of the object buried between the two surfaces GPILE(S+O+S) around $T_{2,\mathrm{S}}$, due to interference between the two indirect contributions of the two buried scaterers, the direct contribution of the lower surface, and as $Q = 1$, one must add the contribution of a round trip of the wave between the object and the lower surface for the direct contribution of the object.

We now take particular care of the depth of the object, denoted as $H_{12}$, and present in the Figs. 4 some scenarios obtained by varying the depth $H_{12}$. The depths are respectively (a) $H_{12} = 24\,\mathrm{mm}$, (b) $H_{12} = 36\,\mathrm{mm}$, (c) $H_{12} = 210\,\mathrm{mm}$ and (d) $H_{12} = 222\,\mathrm{mm}$. If, on the one hand, we consider the case where the object is very close to the upper surface (Figs. 4(a) and (b)), it can happen that the first echo from the upper surface overlaps with the second echo from the object (i.e. $T_{2,\mathrm{O}} \approx T_1$ when $H_{12}$ is very small), thus giving in a first case a constructive interference which results in a single peak of greater amplitude, like in the Fig. 4(a); and in a second case, destructive interference like in Fig. 4(b). These interferences also explain the time lag observed around $T_1$ in these two figures.

If, on the other hand, the object is very close to the lower surface, then the direct and indirect contributions of the object occur almost at the same time as those of the lower surface. Such a scenario is more complex than the first case. Indeed, as $T_{2,\mathrm{O}}$ and $T_{2,\mathrm{S}}$ are very close, the direct and indirect contributions of the two buried scatterers overlap, and create interferences (constructive and/or destructive) which complicate the interpretation of the GPILE results. Moreover, the four contributions to the order $q = 0$ arrive almost at the same time as their resultants to the order $q = 1$. It follows that the GPILE 1/1 signal consists of eight echoes, which contribute and interfere around $T_{2,\mathrm{S}}$. Figs. 4(c)–(d) present such scenarios, where we observe a constructive interference around $T_{2,\mathrm{S}}$ in Fig. 4(c) and destructive/constructive interferences around $T_{2,\mathrm{S}}$ in Fig. 4(d).

Now consider the case of an object buried in a thin layer. Let $H = 54\,\mathrm{mm}$, this scenario being chosen so as to minimize the interferences between the two surfaces. Indeed, we present the scattered fields in this case in Figs. 5, where we observe a weak constructive interference between the echoes of the two surfaces. First, the depth of the object $H_{12} = 24\,\mathrm{mm}$ (like in Fig. 4(a)) and the distance from the object to the lower surface $H_{23} = 30\,\mathrm{mm}$ (like in Fig. 4(c)). For this scenario, the scattered field is presented in Fig. 5(a), where we observe constructive interferences around $T_1$ and $T_{2,\mathrm{S}}$. In the second case, the depth of the object $H_{12} = 36\,\mathrm{mm}$ (like in Fig. 4(b)) and the distance from the object to the lower surface $H_{23} = 18\,\mathrm{mm}$ (like in Fig. 4(d)). For this scenario, we observe destructive interferences around $T_1$ and constructive interferences around $T_{2,\mathrm{S}}$, as shown in Fig. 5(b).

It is valuable to note that in the cases presented respectively in 5(a) and 5(b), the amplitude of the GPILE signal is greater around $T_{2,\mathrm{S}}$ than the scenarios described respectively in 4(c) and 4(d), even though the object is equidistant from the lower surface in 4(c) and 5(a), and in 4(d) and 5(d). In fact, since the object is so close to the two surfaces in 5(a) and 5(b), interferences occur between the two contributions of the object and those of the lower surface around $T_{2,\mathrm{O}}$ and $T_{2,\mathrm{S}}$. Thus, these interferences being constructive for this scenario, this translates into a larger amplitude for the echo of the object buried under the surface, which explains why the GPILE signal has a larger amplitude around $T_{2,\mathrm{S}}$ in the two cases presented in Figs. 5.

In all cases, the nature of interference can change depending on the permittivity or the size of the object for the same depth. For example, if we consider an object of permittivity equal to $\epsilon_{r,2} = 1$ rather than $\epsilon_{r,2} = 7$ as in Figs. 4, we obtain interferences contrary to those observed in Figs. 4. For the size of the object, consider an object whose depth is $H_{12} = 36\,\mathrm{mm}$ as in Fig. 4(b), but whose semi-minor axis is 22 mm instead of 10 mm as in Fig. 4(b), the interferences are constructive and not destructive as in Fig. 4(b). The explanation for this change is that although the two objects have the same depth, the second has a vertex closer to the upper surface than the first, and we know that the direct echoe of the object also depends on its height.

Furthermore, the GPILE method being a generalization of the PILE method (for the case of two scatterers where only one is illuminated) and the EPILE method (for the case of two illuminated scatterers) to the case of an object buried between two rough surfaces, the existence of interferences can also be observed in the case of a scattering by two scatterers. For the case of an object buried under a surface or that of two superimposed surfaces, only the interferences related to the geometry of the problem occur. For example, in Figs. 4, the PILE(S+O) method, which represents the scattered field by the object buried under the surface, shows interferences between the echo of the surface and those of the object, because the object is close to the surface. Similarly, Figs. 5 show the interferences between the echoes of the two surfaces (see PILE (S+S)).

On the other hand, for the case of an object above a surface or for two illuminated objects, the interferences are of the two kinds: those related to the geometry of the problem and those which are present whatever the scenario. Indeed, in the intermediate medium, $\Omega_1$, the GPILE(S+O+S) method for the scattering by the object buried between two surfaces corresponds to the EPILE(O+S) method for the scattering by the object above

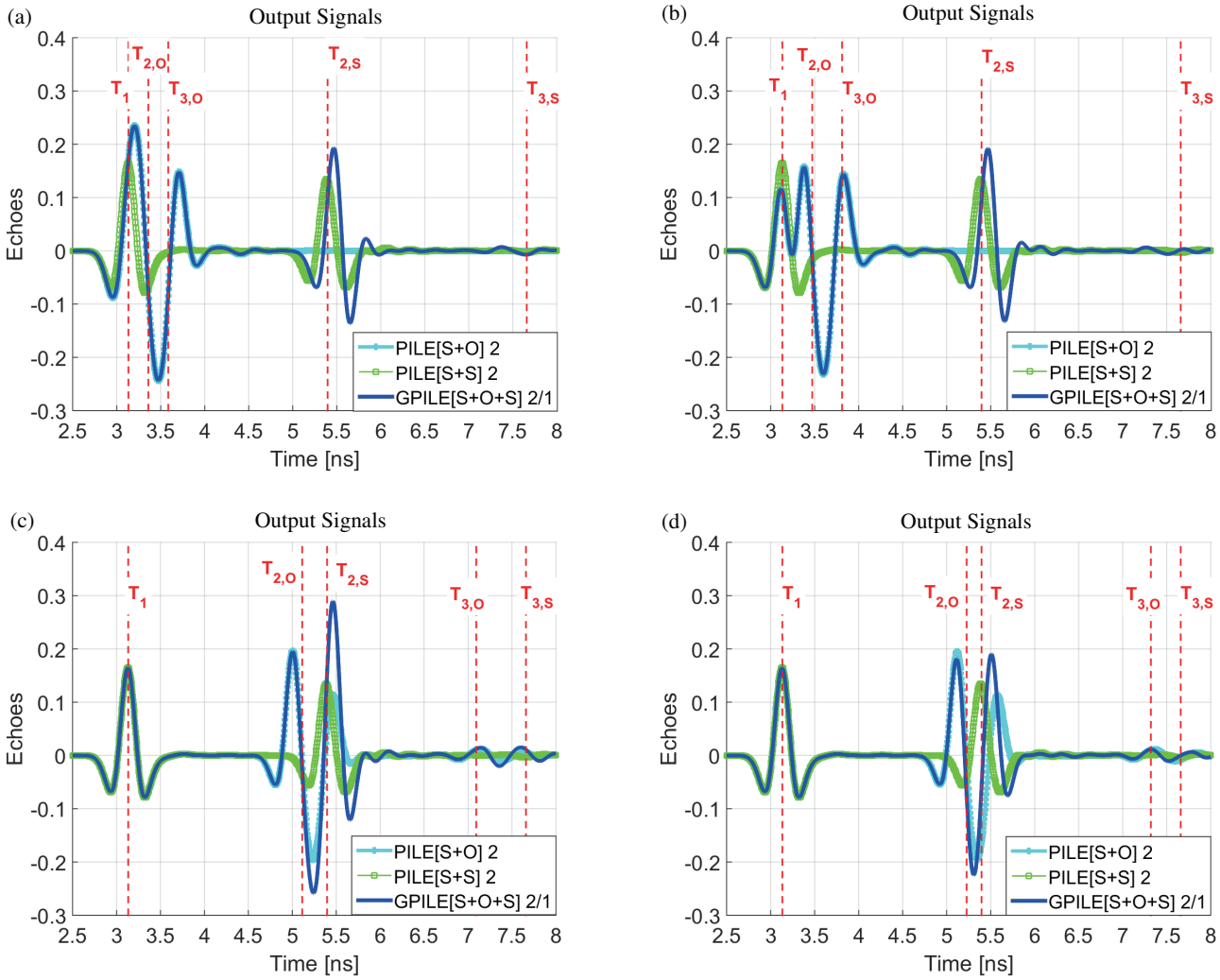


**FIGURE 4**. Time responses of the scattered field, with $x_{\text{obs}} = 0$ and $z_{\text{obs}} = 470\,\text{mm}$. The surface parameters are the same as in Fig. 3. The depth $H_{12}$ of the object varies as a fraction of the thickness $H = 240\,\text{mm}$ between these interfaces. (a) $H_{12} = 24\,\text{mm}$. (b) $H_{12} = 36\,\text{mm}$. (c) $H_{12} = 210\,\text{mm}$. (d) $H_{12} = 222\,\text{mm}$.

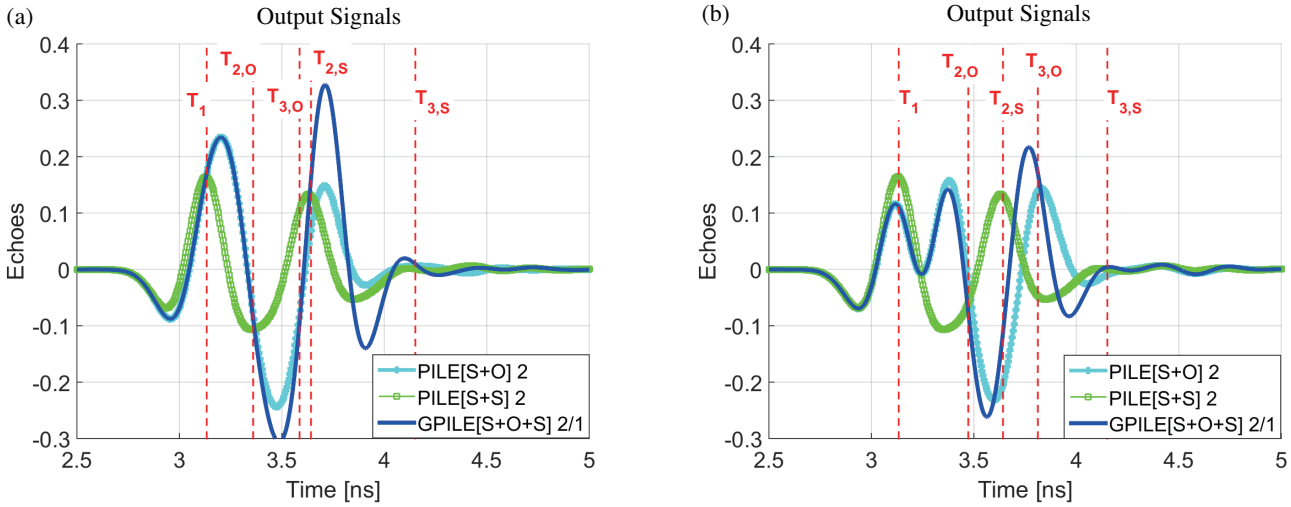


**FIGURE 5**. Time responses of the scattered field, with $x_{\text{obs}} = 0$ and $z_{\text{obs}} = 470\,\text{mm}$. The surface parameters are the same as in Fig. 4, except of the thickness between the two surfaces $H = 54\,\text{mm}$. The depth $H_{12}$ of the object varies. (a) $H_{12} \cong 24\,\text{mm}$. (b) $H_{12} \cong 36\,\text{mm}$.

the lower surface, whose incident field is the field transmitted by the upper surface. Thus, to show examples of interferences in the case of two illuminated scatterers, it suffices to reanalyze Figs. 4 and 5 around $T_{2,S}$. Indeed, when the object is far from the lower surface, we can see the interferences between the indirect contribution of the object and the two contributions of the lower surface. For an object close to the lower surface, there are interferences between the contributions of the two buried scatterers as shown in Figs. 5.

## 5. CONCLUSION

We have used the advantage of the GPILE method, namely to highlight the successive echoes of the three scatterers, to study interferences coming from echoes which constitute the global signal of the GPR response for the case of an object buried between two rough surfaces. We showed that there are two categories of interferences, i.e., those which are present in whatever the chosen scenario, and those which are linked to the geometry of the problem. We then attached special attention to the variation of the depth of the object and showed that when the object is close to one of the two surfaces, there are interference between the echoes of the object and those of the surface. Indeed, when the layer between the two surfaces is relatively thin, the object is close to both surfaces and the problem becomes even more complex.

Moreover, this study can be adapted to all cases of scattering by three interfaces where only one is illuminated, including the scattering by two objects buried under a surface. In this case, the problem will be also complex and several interferences will arise, example given, for an object close to the surface but far from the other object, for two objects that are close to each other but far from the surface, for two objects close to the surface but far from each other, for two objects close to each other and close to the surface, and finally for two objects that have the same depth.

The exploration of interferences between the echoes of three scatterers is a necessary tool for studying the electromagnetic wave scattering from objects buried in a thin layer, like cracks buried under the base of a road. This necessitates the adaptation of physical and geometrical properties of the object to that of a crack buried under the road surface. This is the object of our future research.

## REFERENCES

[1] Yee, K. S., "Numerical solution of initial boundary value problems involving maxwells equations in isotropic media," *IEEE Transactions on Antennas and Propagation*, Vol. AP14, No. 3, 302–307, 1966.

[2] Giannopoulos, A., "Modelling ground penetrating radar by GprMax," *Construction and Building Materials*, Vol. 19, No. 10, 755–762, Dec. 2005.

[3] Déchamps, N., N. de Beaucoudrey, C. Bourlier, and S. Toutain, "Fast numerical method for electromagnetic scattering by rough layered interfaces: propagation-inside-layer expansion method," *Journal of The Optical Society of America A-optics Image Science and Vision*, Vol. 23, No. 2, 359–369, Feb. 2006.

[4] Kubické, G., C. Bourlier, and J. Saillard, "Scattering by an object above a randomly rough surface from a fast numerical method: extended pile method combined with FB-SA," *Waves in Random and Complex Media*, Vol. 18, No. 3, 495–519, 2008.

[5] El-Shenawee, M., "Scattering from multiple objects buried beneath two-dimensional random rough surface using the steepest descent fast multipole method," *IEEE Transactions on Antennas and Propagation*, Vol. 51, No. 4, 802–809, Apr. 2003.

[6] El-Shenawee, M. and C. Rappaport, "Electromagnetic scattering interference between two shallow objects buried under 2-D random rough surfaces," *IEEE Microwave and Wireless Components Letters*, Vol. 13, No. 6, 223–225, Jun. 2003.

[7] El-Shenawee, M., "Polarimetric scattering from two-layered two-dimensional random rough surfaces with and without buried objects," *IEEE Transactions on Geoscience and Remote Sensing*, Vol. 42, No. 1, 67–76, Jan. 2004.

[8] Liang, Y., L. Guo, and Z. Wu, "The EPILE combined with the generalized-FBM for analyzing the scattering from targets above and on a rough surface," *IEEE Antennas and Wireless Propagation Letters*, Vol. 9, 809–813, 2010.

[9] Guo, L., Y. Liang, and Z. Wu, "A study of electromagnetic scattering from conducting targets above and below the dielectric rough surface," *Optics Express*, Vol. 19, No. 7, 5785–5801, Mar. 2011.

[10] Liang, Y., L.-X. Guo, and Z.-S. Wu, "The fast EPILE combined with FBM for electromagnetic scattering from dielectric targets above and below the dielectric rough surface," *IEEE Transactions on Geoscience and Remote Sensing*, Vol. 49, No. 10, 2, 3892–3905, Oct. 2011.

[11] Bourlier, C., C. Le Bastard, and V. Baltazart, "Generalization of pile method to the EM scattering from stratified subsurface with rough interlayers: Application to the detection of debondings within pavement structure," *IEEE Transactions on Geoscience and Remote Sensing*, Vol. 53, No. 7, 4104–4115, Jul. 2015.

[12] Songolo, M., N. Pinel, and C. Bourlier, "Full wave modeling of electromagnetic scattering by an object buried between two rough surfaces: Application to GPR," *Progress In Electromagnetics Research B*, Vol. 96, 133–152, Sep. 2022.

[13] Songolo, M., N. Pinel, and C. Bourlier, "Rigorous numerical method for electromagnetic scattering by an object buried between two rough surfaces," in *2021 IEEE International Geoscience and Remote Sensing Symposium IGARSS*, 3522–3525, 2021.